nature climate change

LETTERS

PUBLISHED ONLINE: 10 MARCH 2013 | DOI: 10.1038/NCLIMATE1835

Attribution of historical ozone forcing to anthropogenic emissions

Drew Shindell[1]*, Greg Faluvegi[1], Larissa Nazarenko[1], Kevin Bowman[2], Jean-Francois Lamarque[3], Apostolos Voulgarakis[1†], Gavin A. Schmidt[1], Olga Pechony[1] and Reto Ruedy[1]

Anthropogenic ozone radiative forcing is traditionally separately attributed to tropospheric and stratospheric changes assuming that these have distinct causes[1]. Using the interactive composition–climate model GISS-E2-R we find that this assumption is not justified. Our simulations show that changes in emissions of tropospheric ozone precursors have substantial effects on ozone in both regions, as do anthropogenic halocarbon emissions. On the basis of our results, further simulations with the NCAR-CAM3.5 model[2], and published studies[3,4], we estimate industrial era (1850–2005) whole-atmosphere ozone forcing of ∼0.5 W m^{-2} due to anthropogenic tropospheric precursors and about −0.2 W m^{-2} due to halocarbons. The net troposphere plus stratosphere forcing is similar to the net halocarbon plus precursor ozone forcing, but the latter provides a more useful perspective. The halocarbon-induced ozone forcing is roughly two-thirds the magnitude of the halocarbon direct forcing but opposite in sign, yielding a net forcing of only ∼0.1 W m^{-2}. Thus, the net effect of halocarbons has been smaller, and the effect of tropospheric ozone precursors has been greater, than generally recognized.

Observations of long-lived greenhouse-gas concentrations are typically used for estimating anthropogenic radiative forcing (RF; defined here as the net radiative imbalance at the tropopause after allowing stratospheric temperatures to respond to an imposed perturbation[1]). Very few reliable historical observations are available for short-lived ozone, however, and thus models are used to estimate changing tropospheric concentrations. Observations extend back several decades in the stratosphere, covering the period when anthropogenic ozone changes are believed to have been greatest. Assessments of RF based on observed ozone depletion in the stratosphere and multi-model simulations of tropospheric changes provide industrial-era ozone RF estimates of ∼0.35 W m^{-2} (range 0.25–0.65 W m^{-2}) due to tropospheric ozone increases and -0.05 ± 0.10 W m^{-2} due to stratospheric ozone loss[1]. Similar results were recently obtained using a merged data set based on models in the troposphere and stratospheric observations[5]. The assumption implicit in separating these regions is that the tropopause is a strong barrier to transport, allowing the areas to evolve independently. However, it is widely recognized that there is significant transport across the tropopause and therefore, prescribing observed changes in one region and using modelled values in the other can lead to inconsistencies.

In simulations using the Goddard Institute for Space Studies GISS-E2-R coupled model, we have included interactive whole-atmosphere ozone chemistry. Although stratospheric trends do not precisely match observations, the links between changes in the troposphere and stratosphere are more consistently represented. To attribute the ozone changes and resulting RFs to underlying causes, we performed simulations driven by changes in only anthropogenic ozone-depleting substances (chlorofluorocarbons (CFCs), hydrochlorofluorocarbons and halons; hereafter ODS) with tropospheric ozone precursors held constant at present-day (∼2005) values; and anthropogenic tropospheric ozone precursor emissions[6] (and methane concentrations) with ODS concentrations fixed at zero. We also analyse simulations made with all historical forcings, which therefore include feedbacks related to climate changes (for example, changes in water vapour or climate-sensitive emissions) whereas the ODS-alone and precursor-alone runs do not.

We calculate RF due to the GISS model's ozone changes using both the GISS radiative transfer model (RTM) and the Community Climate System Model (CCSM4) RTM (these calculations of radiant energy fluxes through the atmosphere have their own distinct base climatology, including clouds, temperatures and water vapour). We find that the whole-atmosphere ozone RF in the all-historical-forcings simulation is 0.17 W m^{-2} using either RTM. Separation of the forcing into that due to tropospheric and stratospheric ozone gave values of 0.26 and −0.09 W m^{-2} using the GISS RTM and the model's internal meteorological tropopause. Calculations with the CCSM4 RTM using the chemical tropopause (150 ppb ozone) yield 0.30 and −0.13 W m^{-2}. These results are consistent with previous studies[1,5].

The GISS-modelled whole-atmosphere ozone changes due to tropospheric precursors produce an RF of 0.34 W m^{-2} whereas those due to ODS changes produce −0.28 W m^{-2} (using the GISS RTM). Values using the CCSM4 RTM were 0.42 and −0.26 W m^{-2}, respectively. Hence, the results are relatively robust to the RTM, although there is some sensitivity for the precursor response, perhaps owing to differences in the location of ozone changes with respect to clouds in the RTMs. The forcing due to ozone precursors peaks in the Northern Hemisphere, with values of 0.4–0.6 W m^{-2} throughout the subtropics and mid-latitudes (Fig. 1). Forcing is substantial worldwide, however, with ∼0.2 W m^{-2} even over most of the remote Southern Ocean. This is consistent with a large role for the well-mixed precursor methane. In contrast, RF due to ODS is concentrated at high latitudes, especially in the Southern Hemisphere associated with the Antarctic ozone hole. This leads to a very inhomogeneous pattern of total all-cause ozone forcing (Fig. 1).

[1]NASA Goddard Institute for Space Studies and Columbia University, New York, New York 10025, USA, [2]NASA Jet Propulsion Laboratory, California Institute of Technology, Pasadena, California 91109, USA, [3]National Center for Atmospheric Research, Boulder, Colorado 80307, USA. †Present address: Department of Physics, Imperial College, London SW7 2AZ, UK. *e-mail: drew.t.shindell@nasa.gov.

© 2013 Macmillan Publishers Limited. All rights reserved.

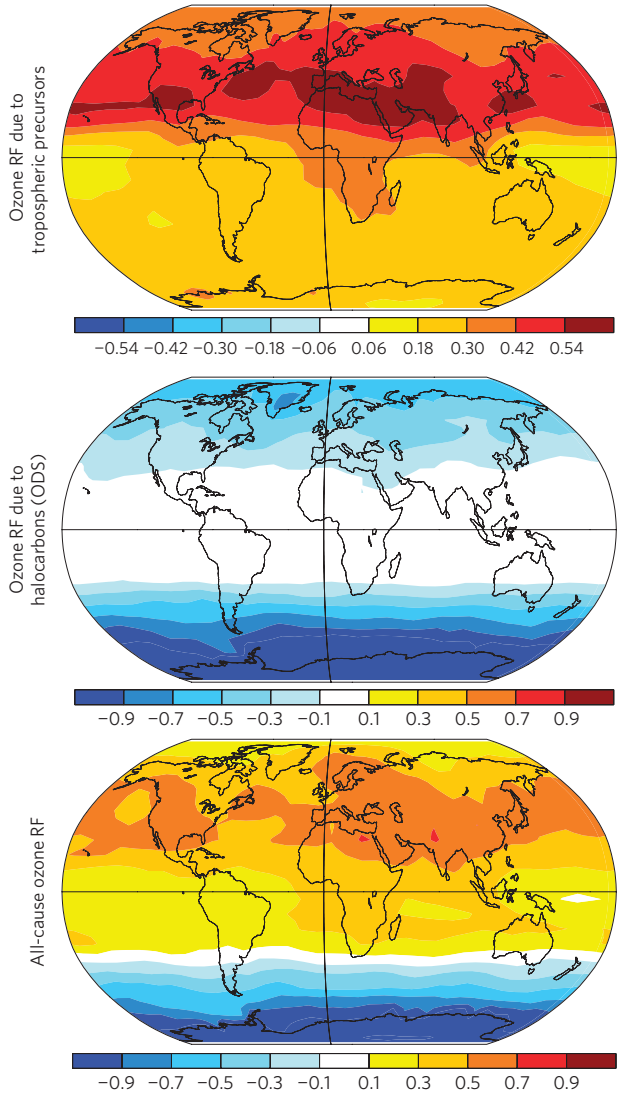

Figure 1 | Annual average whole-atmosphere ozone radiative forcing ($W\,m^{-2}$) due to the indicated drivers from GISS RTM calculations.

Analogous simulations were performed with the National Center for Atmospheric Research Community Atmospheric Model NCAR-CAM3.5 composition–climate model[2] (including the CCSM4 RTM). These produce an ozone RF due to precursors of $0.61\,W\,m^{-2}$. Although that model also examined the ozone RF due to ODS, it produces an Antarctic ozone hole much smaller than observed[7], so we do not include those results in this analysis. A recent study with an independent chemistry model spanning the troposphere and stratosphere, with a similar configuration of reaction rates and modelling set-up, found whole-atmosphere ozone RFs of $0.52\,W\,m^{-2}$ from precursors and $-0.26\,W\,m^{-2}$ from ODS (ref. 3). Finally, tropospheric ozone burden changes of 10.5–11.6 Dobson Units (DU) due to precursor emissions were reported in four models[4]. The impact of these changes on forcing is estimated using a multi-model mean normalized radiative forcing of $0.042\,W\,m^{-2}$ per DU (ref. 8), yielding a range of 0.44–$0.49\,W\,m^{-2}$ due to tropospheric precursors. Although this estimate is only approximate, the results are clearly within the range seen in our analyses.

Forcings are influenced by biases in modelled trends, which are in some cases closely related to biases in the model's present-day ozone climatology. The ozone climatology for the GISS-E2-R model has biases for total column ozone that are largest at Southern Hemisphere middle to high latitudes (Fig. 2, see Methods). Ozone RF depends strongly on the vertical structure of the trends[9], so column biases do not translate directly to forcing biases. Although long-term observations of the full vertical structure do not exist, we use the vertical information in Tropospheric Emission Spectrometer (TES) data[10] to adjust for present-day model biases in areas where those biases can be attributed to overestimates in long-term trends (Fig. 3, see Methods). This reduces forcing magnitudes by 0.07 and $0.01\,W\,m^{-2}$ for ODS and precursors, respectively.

Table 1 | RF by region and driver ($W\,m^{-2}$).

	Whole-atmosphere	Troposphere	Stratosphere
Ozone precursors (through ozone)	0.47 ± 0.14	0.41	0.06
ODS (through ozone)	-0.23 ± 0.07	-0.06	-0.17
Net ozone RF	0.25 ± 0.15	0.35	-0.10
ODS (through direct greenhouse effect)	0.32 ± 0.03		
Net ODS	0.09 ± 0.07		

Precursors are anthropogenic tropospheric precursors, including nitrogen oxides, carbon monoxide, methane and non-methane hydrocarbons. Values are best estimates based on multiple sources as discussed in the text except for troposphere and stratosphere, which are the relative contributions in the GISS model using the meteorological tropopause (although ref. 3 found extremely similar ratios).

We suggest a best estimate for the ozone RF due to precursors of $0.47 \pm 0.14\,W\,m^{-2}$ on the basis of the mean and range from GISS TES-adjusted results using GISS and CCSM4 RTMs, NCAR-CAM3.5 results and ref. 3 (that is, 0.33, 0.41, 0.61 and $0.52\,W\,m^{-2}$). The ODS-induced ozone RF is $-0.23 \pm 0.07\,W\,m^{-2}$ on the basis of the mean of our GISS TES-adjusted RF and ref. 3, with the range incorporating uncertainty based on the magnitude of bias corrections at high Southern latitudes. An overall summary of the effect of each causal agent is presented in Table 1.

The difference between the all-cause ozone forcing and the forcing due to ODS and ozone precursors separately includes the effects of other compounds and feedbacks on composition due to twentieth-century climate change. Climate feedbacks account for 0.01–$0.11\,W\,m^{-2}$ forcing from GISS-modelled industrial era concentration changes (depending on the RTM used). In the NCAR-CAM3.5 model, climate feedbacks cause ozone forcing of $-0.08\,W\,m^{-2}$, whereas previously reported[4] values are 0.07, -0.03 and $0.01\,W\,m^{-2}$. The mean of these results is near zero, but the uncertainty is significant.

Our results are broadly consistent with previous estimates based on tropospheric and stratospheric changes when comparing the effects of similar processes. Roughly 25% of the ODS-induced ozone forcing takes place in the troposphere, resulting nearly equally from decreased transport of stratospheric ozone and from ozone destruction in the uppermost troposphere. Hence, stratospheric forcing is only a portion of the total ODS-induced ozone impact and tropospheric forcing is less than the total amount due to precursors owing to the influence of ODS. The influence of ODS on tropospheric ozone has been overlooked in many previous calculations using separate domains, suggesting that those results were systematically biased high by $\sim$0.05–$0.10\,W\,m^{-2}$. Similarly, $\sim$10–20% of the precursor forcing results from stratospheric ozone changes, primarily ($\sim$75%) due to transport of air with increased ozone into the lowermost stratosphere. Over recent decades this partially masks ODS-induced losses. Although the net ozone forcing ($\sim 0.25\,W\,m^{-2}$) is the same when attributed to region or emissions,

© 2013 Macmillan Publishers Limited. All rights reserved.

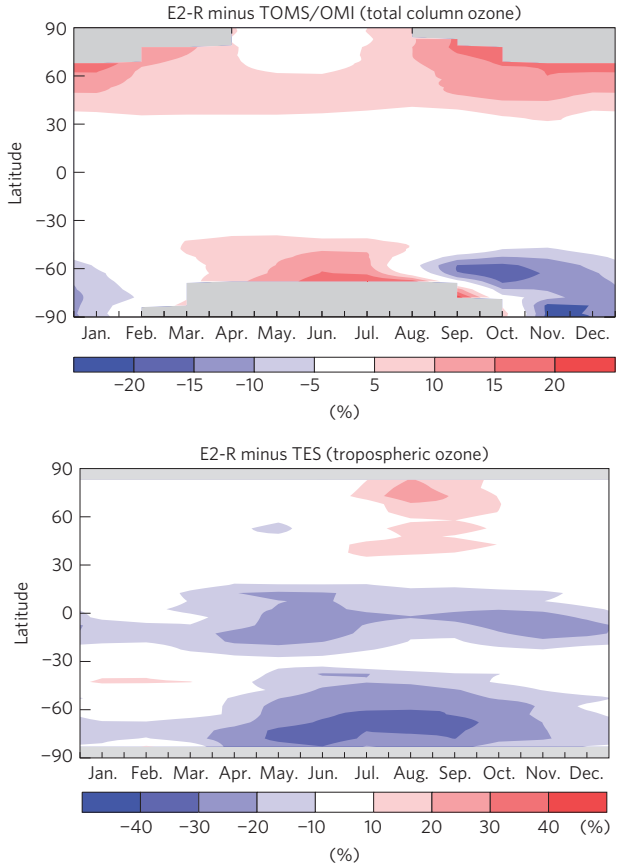

Figure 2 | Differences in modelled ozone versus satellite observations. Comparisons are shown for averages over 2000–2010 for Total Ozone Mapping Spectrometer (TOMS)/Ozone Monitoring Instrument (OMI) total column data (top) and 2005–2009 for TES tropospheric column data (bottom).

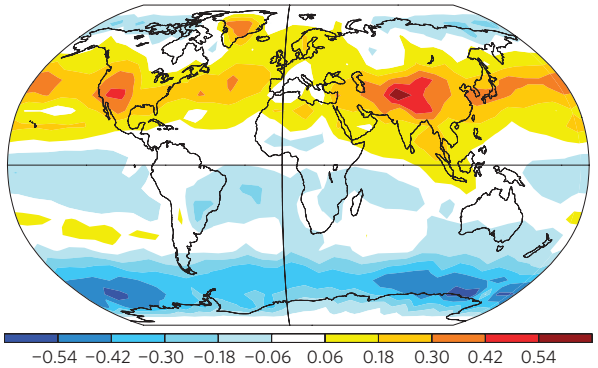

Figure 3 | Difference in annual average radiative forcing (W m^{-2}) between the GISS-E2-R model's ozone and observed TES ozone throughout the atmosphere.

forcing attributable to ozone precursors is roughly one-third greater than that attributable to tropospheric ozone whereas the impact of ODS on ozone is roughly double that attributable to stratospheric ozone (Table 1).

The direct greenhouse RF for ODS (ref. 1) is 0.32 ± 0.03 W m^{-2}. Combining this with our ozone RF results, the ODS have a net impact of only 0.09 ± 0.07 W m^{-2}. This contrasts starkly with the results presented previously[1], which attributed an indirect stratospheric ozone impact of only -0.04 W m^{-2} to these emissions, leading to positive net ODS RF roughly three times our value.

Although we find that the net impact of historical ODS emissions is small, that does not invalidate the widespread notion that the Montreal Protocol (limiting production of ODS) has been successful in preventing warming. This is because ozone depletion would have saturated in polar regions, where it is already near 100% at some altitudes (although it might eventually have become large in the tropics with very large CFC loading[11]), and direct halocarbon RF would have grown steadily to be a further ~0.5 by 2020 and well over 1 W m^{-2} later in the century[12]. To examine this issue, we performed another experiment using the same model in which CFCs were set to 2050 levels following a hypothetical world-avoided scenario[11] under which CFCs were not regulated. In this simulation, the CFC direct RF was 2.3 W m^{-2} whereas RF due to the induced ozone changes was 0.14 W m^{-2} relative to 2000. Ozone forcing was near zero at Southern Hemisphere middle and high latitudes, indicating saturation where chemical losses are already large, whereas a strong negative forcing (>2.0 W m^{-2}) took place over the Arctic. This was offset, however, by a weak but broad positive low-latitude forcing. Thus, limiting ODS emissions has indeed been beneficial for mitigating future climate change.

Our results imply that reducing emissions of ozone precursors may have greater benefits than previously recognized. Analysis of forcings based on emissions rather than concentration changes, and consistently modelling the whole atmosphere, provides further insight into the drivers of climate change and substantially more useful policy-relevant information.

Methods

Observations used in model evaluation. We use a TES ozone climatology covering 2005–2009. TES data typically have fairly small positive biases throughout the troposphere, usually ~3–10 ppb (ref. 13), and reproduce the total column seen by other measurements well[10]. Long-term total column trends are evaluated from 1980 to 2009 using the ERA-interim satellite-based reanalysis product[14]. Northern Hemisphere surface ozone data are from a variety of individual stations, including several at mountain-top observatories sampling the free troposphere. Note that uncertainties in the measured surface trends are large[6,15–17].

GISS model biases. In the GISS model, present-day zonal mean total column ozone[18] or tropospheric column ozone[10] biases in the tropics and Northern Hemisphere are always less than 20% (Fig. 2), and total column ozone trends over 1980–2000 are statistically in agreement with observations[15]. Modelled long-term Northern Hemisphere surface ozone trends are also generally consistent with observed increases or underestimated[6,15–17]. At middle to high Southern Hemisphere latitudes, the model shows tropospheric ozone column biases up to −35% (Fig. 2) and overestimates total column decreases[14] (although much of this is during seasons with little sunlight, and the trends themselves have substantial uncertainties). High-latitude Southern Hemisphere springtime losses extend too far equatorward, consistent with the total column biases (Fig. 2), and are too large in the lowermost stratosphere[15,19]. This seems to result from cold biases near the tropopause at Southern Hemisphere middle to high latitudes causing exaggerated chemical ozone losses during cold seasons when polar stratospheric clouds are present.

Calculation of RF biases. The bias in the modelled Southern Hemisphere middle- to high-latitude total column trend is almost identical (ratio 1.08) to the bias in the present-day total column versus TES, suggesting that the TES–model differences are almost entirely attributable to trend overestimates rather than systematic biases in the model. We therefore assume that the model Southern Hemisphere biases are due to overestimates of depletion by ODS, and use the vertical TES–model differences to adjust for these biases.

We first calculate the RF due to the difference between the modelled and TES present-day total natural plus anthropogenic ozone (Fig. 3). We calculate the RF using GISS model and TES ozone both throughout the atmosphere and also below the model's internally calculated tropopause. The global mean whole-atmosphere ozone RF difference is 0.007 W m^{-2}, whereas the tropospheric ozone RF difference is 0.016 W m^{-2}. The good global mean agreement in part results from a cancellation of positive biases in the Northern Hemisphere and negative biases in the Southern Hemisphere, which are 0.12 and −0.11 W m^{-2}, respectively, for whole-atmosphere ozone RF (Fig. 3). These large-scale biases are nearly identical for tropospheric ozone forcing, indicating that they are driven by differences in tropospheric rather than stratospheric ozone, consistent with our earlier model evaluation[15].

© 2013 Macmillan Publishers Limited. All rights reserved.

We then use these TES–model RF differences to correct for model Southern Hemisphere biases. We adjust the annual average forcing due to ODS-induced ozone decreases in the troposphere by subtracting the model's $-0.31\,W\,m^{-2}$ bias in 45°–90° S tropospheric ozone forcing (Fig. 3), which reduces the estimated ODS-induced global mean ozone RF from -0.28 to $-0.24\,W\,m^{-2}$ (accounting for the relative area from 45°–90° S). The tropospheric ozone forcing due to ODS including this adjustment is $-0.06\,W\,m^{-2}$. Using the model/TES whole-atmosphere ozone RF bias instead lowers the RF to $-0.21\,W\,m^{-2}$, implying an overestimate of $\sim 0.03\,W\,m^{-2}$ due to stratospheric ozone losses. Thus, although Southern Hemisphere middle to high latitude biases in total column trends during the satellite era (through 2009) are 50–60%, their impact on global mean RF due to ODS is much smaller (25%) owing to their occurrence primarily during polar night and over a small area. A calculation using TES instantaneous radiative kernels[20] (IRK) finds tropospheric ozone RF differences for the Southern Hemisphere extratropics of only $\sim 0.03\,W\,m^{-2}$. As that calculation used the 150 ppb ozone contour to define the tropopause, the smaller value indicates that forcing biases come largely from the tropopause region (above the 150 ppb contour, but below the meteorological tropopause), suggesting that they are indeed linked to ODS in the stratosphere. The TES-adjusted RFs due to ODS are comparable in the two hemispheres (-0.12 and $-0.09\,W\,m^{-2}$ global mean forcing due to Southern Hemisphere and Northern Hemisphere ozone, respectively), consistent with observed ozone mass trends, and the total of $-0.21\,W\,m^{-2}$ is in reasonable agreement with an independent study[3], suggesting that this result is fairly robust.

In the Northern Hemisphere, extratropical biases calculated using TES tropospheric IRKs ($\sim 0.04\,W\,m^{-2}$) are much smaller than the $0.14\,W\,m^{-2}$ biases using the GISS RTM and the meteorological tropopause, suggesting that most of the latter is also related to the stratosphere and not to surface emissions. Furthermore, Northern Hemisphere positive biases seem to have a substantial systematic component because, as noted, modelled surface trends are generally correct or observed increases are underestimated. Hence, in the Northern Hemisphere we adjust the precursor impact by subtracting only the small TES IRK-based difference, leaving an RF of $0.33\,W\,m^{-2}$ ($0.41\,W\,m^{-2}$ using the CCSM4 RTM results).

Received 1 August 2012; accepted 23 January 2013; published online 10 March 2013

References

1. Forster, P. *et al.* in *IPCC Climate Change 2007: The Physical Science Basis* (eds Solomon, S. *et al.*) 129–234 (Cambridge Univ. Press, 2007).
2. Lamarque, J. *et al.* CAM-chem: Description and evaluation of interactive atmospheric chemistry in the community Earth system model. *Geosci. Model Dev.* **5,** 369–411 (2012).
3. Sovde, O., Hoyle, C., Myhre, G. & Isaksen, I. The HNO_3 forming branch of the $HO_2 + NO$ reaction: Pre-industrial-to-present trends in atmospheric species and radiative forcings. *Atmos. Chem. Phys.* **11,** 8929–8943 (2011).
4. Gauss, M. *et al.* Radiative forcing since preindustrial times due to ozone change in the troposphere and the lower stratosphere. *Atmos. Chem. Phys.* **6,** 575–599 (2006).
5. Cionni, I. *et al.* Ozone database in support of CMIP5 simulations: Results and corresponding radiative forcing. *Atmos. Chem. Phys.* **11,** 11267–11292 (2011).
6. Lamarque, J-F. *et al.* Historical (1850–2000) gridded anthropogenic and biomass burning emissions of reactive gases and aerosols: Methodology and application. *Atmos. Chem. Phys.* **10,** 7017–7039 (2010).
7. Austin, J. *et al.* Chemistry-climate model simulations of spring Antarctic ozone. *J. Geophys. Res.* **115,** D00M11 (2010).
8. Ramaswamy, V. *et al.* in *IPCC Climate Change 2001: The Scientific Basis* (ed. Houghton, T.) 349–416 (Cambridge Univ. Press, 2001).
9. Lacis, A., Wuebbles, D. J. & Logan, J. A. Radiative forcing of climate by changes in the vertical distribution of ozone. *J. Geophys. Res.* **95,** 9971–9981 (1990).
10. Osterman, G. B. *et al.* Validation of tropospheric emission spectrometer (TES) measurements of the total, stratospheric, and tropospheric column abundance of ozone. *J. Geophys. Res.* **113,** D15S16 (2008).
11. Newman, P. *et al.* What would have happened to the ozone layer if chlorofluorocarbons (CFCs) had not been regulated? *Atmos. Chem. Phys.* **9,** 2113–2128 (2009).
12. Velders, G., Andersen, S., Daniel, J., Fahey, D. & McFarland, M. The importance of the Montreal Protocol in protecting climate. *Proc. Natl Acad. Sci. USA* **104,** 4814–4819 (2007).
13. Nassar, R. *et al.* Validation of tropospheric emission spectrometer (TES) nadir ozone profiles using ozonesonde measurements. *J. Geophys. Res.* **113,** D15S17 (2008).
14. Dee, D. *et al.* The ERA-Interim reanalysis: Configuration and performance of the data assimilation system. *Q. J. R. Meteorol. Soc.* **137,** 553–597 (2011).
15. Shindell, D. T. *et al.* Interactive ozone and methane chemistry in GISS-E2 historical and future climate simulations. *Atmos. Chem. Phys.* (in the press).
16. Oltmans, S. *et al.* Long-term changes in tropospheric ozone. *Atmos. Environ.* **40,** 3156–3173 (2006).
17. Parrish, D. D., Millet, D. B. & Goldstein, A. H. Increasing ozone in marine boundary layer inflow at the west coasts of North America and Europe. *Atmos. Chem. Phys.* **9,** 1303–1323 (2009).
18. McPeters, R. *et al.* Validation of the aura ozone monitoring instrument total column ozone product. *J. Geophys. Res.* **113,** D15S14 (2008).
19. Randel, W. & Wu, F. A stratospheric ozone profile data set for 1979–2005: Variability, trends, and comparisons with column ozone data. *J. Geophys. Res.* **111,** D06313 (2007).
20. Worden, H., Bowman, K., Kulawik, S. & Aghedo, A. Sensitivity of outgoing longwave radiative flux to the global vertical distribution of ozone characterized by instantaneous radiative kernels from Aura-TES. *J. Geophys. Res.* **116,** D14115 (2011).

Acknowledgements

We thank NASA MAP for financial support and the NCCS for computer services.

Author contributions

G.F. performed the GISS composition simulations, L.N. and R.R. performed the GISS RTM calculations, K.B. facilitated use of the TES data, J-F.L. performed the NCAR simulations, A.V., G.A.S., O.P. and D.S. contributed to developing and evaluation the GISS composition model, D.S. conceived and led the study, and all authors contributed to writing the paper.

Additional information

Reprints and permissions information is available online at www.nature.com/reprints. Correspondence and requests for materials should be addressed to D.S.

Competing financial interests

The authors declare no competing financial interests.

© 2013 Macmillan Publishers Limited. All rights reserved.